LANGMUIR

pubs.acs.org/Langmuir Article

# Predicting the Splash of a Drop Impacting a Thin Liquid Film

S. Rajendran, M. A. Jog, and R. M. Manglik*

Cite This: *Langmuir* 2023, 39, 14764−14773 Read Online

ACCESS | Metrics & More | Article Recommendations

**ABSTRACT:** An experimental study is carried out to investigate droplet−film interactions when a drop impinges on a thin stagnant film of the same liquid. The impacting drop causes either liquid deposition or splash, consisting of prompt generation of secondary drops or a delayed process. By varying the drop diameter and impact velocity, measurements are made to characterize the phenomena using five different liquids that are chosen to cover a wide range of liquid properties (viscosity and surface tension). The drop impact dynamics are captured with a high-speed digital camera with real-time, high-resolution image processing. The drop-splash threshold is found to scale with inertial and viscous forces, or Reynolds number (Re), as well as capillary forces, as described by the balance of gravitational and interfacial tension forces, or Bond number (Bo); fluid properties are described by their Morton number (Mo). A correlation, functionally expressed as $Re = \phi(Bo,Mo)$, is devised to determine the splash/no-splash (or deposition) boundary, and the predictions for the splash/no-splash outcomes agree well with the experimental outcomes as well as those readily available in the literature.

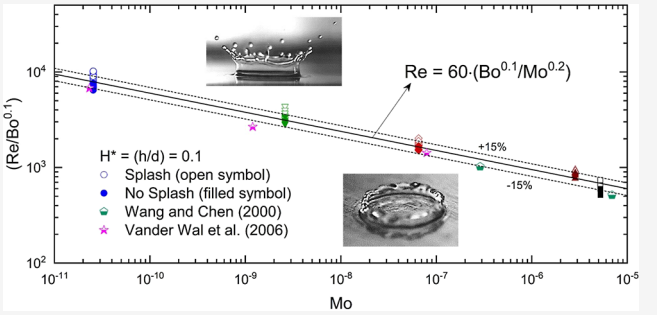




## INTRODUCTION

The significance of advancing the understanding of drop impingement interactions on thin liquid layers extends to spray-based coatings, painting, cleaning, inkjet printing, and metal and alloy quenching. Drop impingement is also a primary mass transport process in spores and microorganism dispersion and pesticide coatings. Because chemicals (biocides, chelating agents, surfactants, and fatty acids, among others) are used in their working liquids, splash-induced airborne secondary droplets engender localized pollution. This environmental contamination has been identified as a chemical and/or biological occupational risk factor leading to dermatological and respiratory ailments, such as increased occurrence of asthma, hypersensitive pneumonitis, and cancer of the esophagus, stomach, larynx, etc.[1] In order to minimize the risks of such outcomes from spray-drop impingement splash, the Occupational Safety and Health Administration (OSHA) and the National Institute of Occupational Safety and Health (NIOSH) have defined permissible exposure limits that the industry is required to comply with.[2] Resolving and understanding the splash and adhesion phenomena of drop impact would therefore assist greatly in exercising better process control in all these multifaceted usages. Devising means to predict and control the splash post-drop impact on its liquid film while maintaining the desired functionality of the associated spray process thus becomes crucial.

In most spray applications, the target surface or substrate may be initially dry, but with continuous drop impact, a thin liquid-film layer is formed on which further impingement occurs with altered dynamics. Deposition of the liquid mass transported by the drops occurs when they merge with the liquid film without generating secondary drops. Depending upon the drop size, liquid-film thickness, and velocity, splatter or splash may occur, which results in the production of secondary drops either at the instant of impact (prompt splash) or through a delayed breakup of the rim of the crown formed as a result of the impact (delayed splash). This droplet−surface impingement phenomenon, with or without a liquid film, is inherently complex, and its physical understanding is far from complete. Worthington[3] was perhaps the first to document in 1876 the resultant patterns created by falling drops of water and mercury on a dry surface. Since then, the efforts to better characterize these phenomena and devise control mechanisms have continued to be a focus of research due to both its practical relevance and innate complexity.[4−13] Some recent experimental studies with high-speed imaging have provided additional insights into the drop impact process.[14−16] Computational or numerical simulations have further explored several distinct features of drop impact

Received: July 31, 2023
Revised: September 12, 2023
Published: September 27, 2023

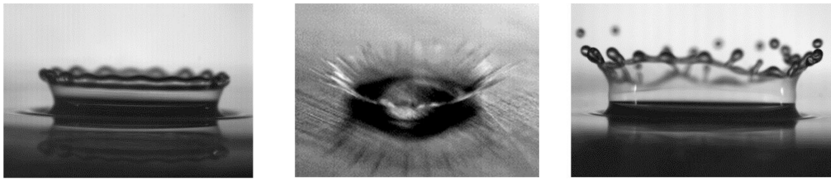


**Figure 1.** Photographic images of liquid-drop impact dynamics on a thin-film of the same liquid showing (a) deposition or no splash with crown formation, (b) prompt splash with crown formation, and (c) crown formation with delayed splash (note that these photos are individually magnified to different scales and should not be used for size estimations, as they are only presented for representation of the deposition or splash outcomes).

(formation, propagation, crown growth, splashing limits, etc.) and the role of drop characteristics such as size, shape, and velocity.[17−21] Because the liquid-drop impingement interactions with the pre-existing thin-film layer are critical for spray process control, its prognostic understanding is further addressed in the present work.

As suggested in drop-impact dynamics reviews,[14,22] the associated kinetics and outcomes are dependent upon a number of parameters: drop size and impact velocity, drop and film liquid properties (density, viscosity, and rheology), interfacial tension, surface properties (roughness, contact angle, and wettability), and thermal properties. When a drop impinges on a thin liquid film, as indicated previously, different regimes of liquid movement occur that are broadly classified as *deposition* or *splashing*. Characteristic representations of these postimpact regimes are illustrated in Figure 1. In *deposition*, the merging of the impacting drop with the liquid film does not produce any secondary drops, which may or may not include capillary surface waves that form a *crown* before merging with the liquid film. Deposition with crown formation is also referred to as *crown-deposition*.[23] When secondary drops are discharged or *splashing* occurs, at certain conditions on impact, an ejected jet is formed at the neck (small region between the drop and the thin film). This jet spreads out and tilts upward, forming a *crown* with unstable rims that break up into secondary drops before dropping down and merging into the thin film. The liquid crown tends to break up at or beyond the expansion of the crown. This has been termed as *delayed* or *crown splashing*; see, for example, the studies reported by Josserand and Zaleski[24] and Deegan et al.[25] In *prompt splash*, which is a supplementary phenomenon that could occur when secondary drops are formed at the instant of drop impact on the thin film, it has been shown[25] that the ejected jet tends to shoot out from underneath the drop parallel to the fluid layer.

One of the earliest attempts to quantify the distinguishing boundary between these drop-impact deposition and splash regimes was reported in 1980 by Walzel.[26] Working with water and two different glycerin−water solutions, drop-impact outcomes on both a hard-clean surface and a thin film were explored. The impinging drop dynamics was characterized by the following force balances

$$\text{Weber number, } We = \left(\frac{\rho v^2 d}{\sigma}\right) = \frac{\text{inertial force}}{\text{surface tension force}} \tag{1}$$

$$\text{Ohnesorge number, } Oh = \left(\frac{\mu}{\sqrt{\rho\sigma d}}\right) = \frac{\text{internal viscosity dissipation}}{\text{surface tension energy}} \tag{2}$$

Note that instead of explicitly using *Oh*, as in eq 2, Walzel[26] had scaled the results in terms of a dimensionless drop diameter, $d^* = (\rho\sigma d/\mu^2)=(1/Oh^2)$. Based on their own impingement outcome data for a relative film thickness of 0.1, which was defined as $(H^* = h/d)$, the demarcation between no-splash and splash events has been given by

$$(We{\cdot}d^{*0.2}) = (We/Oh^{0.4}) = K = 2500 \tag{3}$$

It must be recognized here that Oh was considered to account for the viscosity of the liquid drop and that it is also linked with *We* and *Re* when expressed as

$$\text{Reynolds number, } Re = \left(\frac{\rho v d}{\mu}\right) = \frac{\text{inertial force}}{\text{viscous force}} = \frac{\sqrt{We}}{Oh} \tag{4}$$

Further recognizing the role of liquid viscosity, Cossali et al.[27] measured the splashing threshold in extended drop-impact experiments that involved, besides water, several different glycerine−water solutions ($0.0022 \le \text{Oh} \le 0.141$) on different target liquid-film surface conditions ($0.1 \le H^* \le 1.0$). They proposed the following correlation in terms of *We*, *Oh*, and $H^*$ to estimate the splashing limit

$$K = (We/Oh^{0.4}) = [2100 + 5880\text{H}^{*1.44}] \tag{5}$$

It should be noted that the parameter *K*, or the scaling with $(We/Oh^{0.4})$ expressed in both eqs 3 and 5, was initially developed to describe drop impact on dry solid surfaces[6,17,22] and has been subsequently adapted for drop impact on liquid films. In a similar effort, by employing multiple viscous liquids, Rioboo et al.[23] have further explored drop impact on thin films and clarified two distinct outcomes of postimpact crown formation, namely, deposition-crown and crown-splash. Their respective limits or thresholds are presented graphically and are seen to be influenced by the film height $H^*$ when the film was very thin ($H^* < 0.06$) but are constant with larger film thicknesses ($0.06 < H^* < 0.15$). For the latter case with crown-splash, the demarcation between deposition and splash is given by

$$K = (We/Oh^{0.4}) = 2100 \tag{6}$$

An important issue in droplet interaction with liquid films is the difficulty in producing and maintaining small film thicknesses. This has been addressed by Wang and Chen,[28]



https://doi.org/10.1021/acs.langmuir.3c02185
Langmuir 2023, 39, 14764−14773

who have explored reliable and repeatable means to produce thin films on a surface. They devised a new technique for maintaining thin films and found that the critical splash level was insensitive to film height when the film is sufficiently thin ($H^* \leq 0.1$). Different concentrations of glycerol−water solutions were used to experimentally delineate distinguishing the splashing criterion. Based on their results for $H^* \leq 0.1$, they identified the critical $We_c$ to demarcate the splash and no-splash boundary for each of the three liquids considered ($0.0175 \leq Oh \leq 0.1030$). $We_c$ has different values with changing liquid viscosity (represented by $Oh$), and no attempt was made to reconcile results with previously reported correlations.[26,27] In a relatively recent study, Vander Wal et al.[29] have presented splash and no-splash results using a variety of different liquids ($0.0029 \leq Oh \leq 0.165$) on a dry surface as well as thin and thick liquid films ($H^* = 0.1$, 1.0, and 10). Experimental results were obtained using a constant diameter droplet ($d = 2.0$ mm) on the dry surface and each of the liquid films with different drop-impact velocities ($v = 1.36$, 2.17, 3.15, and 3.80 m/s). They too have neither compared their data with predictions of previous correlations nor attempted to devise differently but conclude that the scaling with $Re$, $We$, and $Oh$ does not lend to any simple correlation. An intriguing observation in this assertion is that the Reynolds number $Re$ is interrelated[30,31] with both $We$ and $Oh$, and the use of all three together may be redundant and thus require a re-evaluation, as in the present work.

Okawa et al.[32] have also carried out experimental measurements with much higher film thicknesses ($0.43 \leq H^* \leq 68$) but have compared them with those of other studies with $H^* \leq 0.1$. They have concluded that while scaling with $K$, or $(We/Oh^{0.4})$, is still applicable, the splash/no-splash demarcation is constant ($K \approx 2100$; same as in[23]) for all film thicknesses, including $H^* = 0.1$. Deegan et al.[25] have also studied the complexities of splashing on a relatively thick liquid film ($H^* = 0.2$) with a variety of liquids (water, propanol, silicon oil, and a glycerol−water solution). Based on their own data, they have suggested the following correlation in terms of $We$ and $Re$ (which has also been re-expressed in terms of $We$ and $Oh$)

$$We \cdot Re^{0.5} = 2.6 \times 10^4; \text{ or } (We/Oh^{0.4}) \simeq 3299 \quad \text{for } H^* = 0.2 \tag{7}$$

This prediction is about 23% higher than the 2679 value obtained from the Cossali et al.[27] correlation in eq 5. Much more recently, Okawa et al.[16] have revisited the drop-splash problem with thick films ($0.2 \leq H^* \leq 3.33$) and a variety of liquids (water, ethanol, water−ethanol, and water−glycerol solutions; $0.00192 \leq Oh \leq 0.03753$). They have developed a correlation for splash thresholds based on these data and found that its extrapolation to $H^* \sim 0.1$ substantially underpredicts the critical $We$ when compared with the Cossali et al.[27] data. A few computational or numerical modeling studies have tried to elucidate the localized features of the drop-impact−liquid-film dynamics. They have primarily explored the behavior with a kinematic discontinuity model,[6,33] propagation of crown formation and film-surface effects,[18] and other such drop-splash dynamical considerations.[17,19−21] These efforts have, however, not yielded predictive models for the onset of splash and its regimes.

The focus of the current study is to revisit this problem of predicting the threshold for postimpingement drop splash on a thin film ($H^* \sim 0.1$) in an effort to redress the previous anomalies. In this context, it is instructive to compare the various predictions for thin films as reviewed in the foregoing, and this is presented in Figure 2. The rather large range of

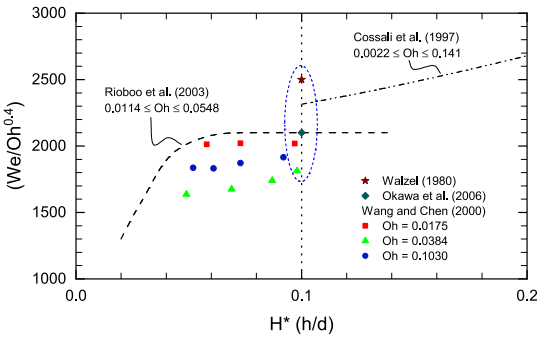


**Figure 2.** Comparison of different correlations[23,27] and data[26,28,32] for the critical value of $K$, or $(We/Oh^{0.4})$, for the onset of splash with drop impingement on liquid films.

predictions, $1812 \leq (We/Oh^{0.4}) \leq 2500$, for the thin film limit of $H^* \leq 0.1$ and the preceding review clearly suggest a re-evaluation of the scaling of the controlling drop-splash dynamics. Another curious aspect of Figure 2 is that $Oh^{0.4}$ does not reconcile the different Oh data of Wang and Chen,[28] which have different values for $(We/Oh^{0.4})$ in each case. Thus, with the objective of resolving the ambiguity and considerable variability of the literature results, the delayed splash of drops on a thin liquid film ($H^* = 0.1$) has been investigated experimentally in this study. Besides water, five other liquids are employed so as to address the significant influence of fluid properties, particularly that of viscosity and surface tension. By producing and maintaining a consistent film of a thickness of $H^* = 0.1$, which represents the limiting case for thin films (Figure 2, and see[22,23,26−29]), we have attempted to understand the underlying physics of the drop-surface−film interaction and reassess the scaling of the associated mechanisms. The latter are shown to be parametrically governed by capillary or surface tension, gravitation or density, and inertial and viscous forces, which are further shown to be appropriately scaled by the Reynolds, Bond, and Morton numbers. Finally, a correlation is devised that has been shown to effectively predict the onset of splash as measured by both the data set of this study and much of those available in the literature.

## EXPERIMENTAL METHODS AND MATERIALS

To experimentally characterize the interactions between a single liquid drop impacting a thin film of the same liquid, the test apparatus and measurement controls are schematically shown in Figure 3. A square acrylic container served as the main observation chamber, and it housed the target surface or substrate and also functioned as the liquid reservoir and collecting tank. The copper target surface was installed inside the center of this container on a raised acrylic platform. The containing walls were made to be large enough to avoid interference with the splashing droplets and to provide for clear viewing of the ensuing postdrop-impact dynamics. Impinging drops were generated at a steady rate from a NEXUS 3000 syringe pump. The change in drop release height along with adjustments to the flow rate provided a range of drop impact velocities. The flow rate was varied from 0.5 to 8.0 mL/min for the different cases measured and characterized experimentally, and this resulted in drop velocities ranging from $v = 1.0$ to 3.0 m/s for drop diameters ranging from $d = 3.5$ to 5.2 mm. The drops were released from a prescribed predetermined height above the target surface through a circular stainless steel needle. The needle was always maintained perpendic-


https://doi.org/10.1021/acs.langmuir.3c02185
Langmuir 2023, 39, 14764−14773

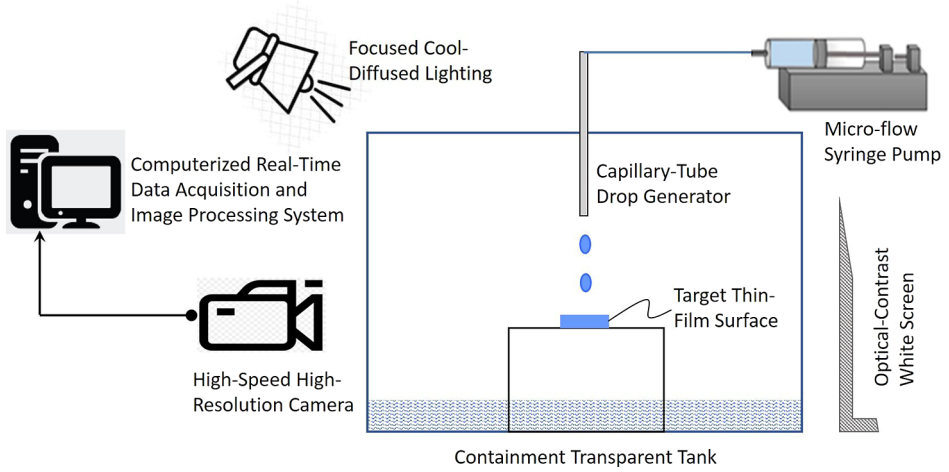


**Figure 3.** Schematic of the experimental set up with a droplet generator, a substrate with thin film, and real-time high-resolution high-speed video image capture and data acquisition.

ular to the target surface using a bubble level. The target surface had no inclination and was maintained parallel to the ground and, hence, perpendicular to the gravitational force. Because this surface was substantially larger than the size of the impacting drop, the increase in film thickness with each impacting drop was found to be negligible and thereby ensuring a constant film thickness.

As has been delineated in the previous section and illustrated in Figure 1, when a single drop impacts a thin liquid film, the outcome may result in either a splash event or in deposition. A range of deposition and splash outcomes could be produced in the experiments by varying the drop size and its impact velocity. Multiple drops of the test liquid were initially impinged on the target surface to obtain a uniform and carefully measured thin film with a $(H^* = h/d) = 0.1$. This film was left undisturbed for a time period sufficient to ensure that no surface undulations exist. Once the thin film was stable, the film thickness was measured using digital imaging processing techniques. An example of an image used for measuring and calibrating liquid film thickness is presented in Figure 4, wherein the thickness was calibrated by using the known needle diameter as the reference. The uniformity of the film was checked by repeating the measurements across different sections of the image. The film so produced on the target surface was maintained in its thickness and left undisturbed prior to recording the drop-impact observations.

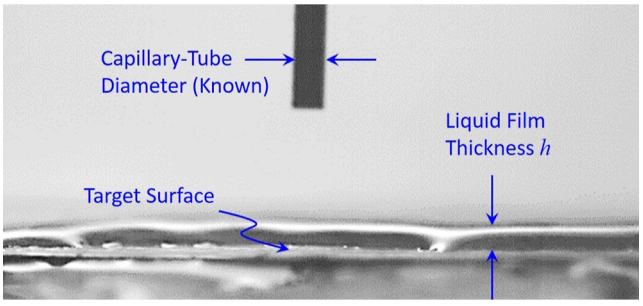


**Figure 4.** Measurement of thin film thickness using high-resolution digital image processing; the known capillary tube or drop-producing needle diameter serves as the calibration for drop size, spread, film thickness, and crown characterization.

To characterize and measure the drop impact on the thin liquid film and the subsequent deposition or splash outcomes, real-time, high-resolution digital videography and image processing was employed. A high-speed digital camera (Hi-D cam—II version 3.0—NAC Image Technology) was used, which was kept in an appropriate viewing orientation. Video images were recorded at a shutter speed of 1/2000 s and a frame rate of 500 fps with the camera placed at about 1.5 ft from the target surface. A single-bulb focusing light system (ARRI) with glossy aluminum reflectors was used to obtain clear and high-contrast images. The light system was focused on a white screen that was placed parallel to the plane of viewing; it is a "cool" lighting system and obviates any significant heating of the immediate environment of the apparatus. The high-resolution images thus obtained were analyzed using image-processing software Image-Pro 4.0 (Media Cybernetics).

The diameter of the impacting drop $d$ was calculated based on the pixel area occupied by the drop in the recorded image. Assuming the drop to be spherical and therefore a circle in the image plane, we calculated the effective diameter from the measured pixel area of the digital image. Drop impact velocity $v$ was determined by comparing the position of drops, prior to impact, in successive frames with respect to a fixed point in the frame. The impact velocity was not constant due to gravitational acceleration and drag force acting on the drop. Therefore, to circumvent this, only three appropriate images immediately prior to impact on the film surface were considered for calculations. For each set of experimental measurements, images were calibrated using the outer diameter of the known diameter of the stainless steel needle used for drop generation. Each experiment was repeated to check for and verify repeatability, and the consequent average measurements are used in the ensuing analysis.

To help us understand the influence of liquid properties on the splashing phenomena, five different liquids with varying properties

**Table 1. Properties of the Different Liquids Used in the Drop-Splash Experiments**

| liquid | density [kg/m$^3$] | viscosity [Pa.s] | surface tension [N/m] | *Mo* [-] |
|---|---|---|---|---|
| Water | 998.0 | $1.00 \times 10^{-3}$ | 0.0728 | $2.55 \times 10^{-11}$ |
| 25% by volume propylene glycol–water (25% PG) | 1007.5 | $2.55 \times 10^{-3}$ | 0.0541 | $2.60 \times 10^{-9}$ |
| 50% by volume propylene glycol–water (50% PG) | 1017.0 | $5.00 \times 10^{-3}$ | 0.0452 | $6.53 \times 10^{-8}$ |
| 75% by volume propylene glycol–water (75% PG) | 1026.5 | $1.20 \times 10^{-2}$ | 0.0411 | $2.85 \times 10^{-6}$ |
| ethylene glycol (EG) | 1113.2 | $1.61 \times 10^{-2}$ | 0.0484 | $5.22 \times 10^{-6}$ |



https://doi.org/10.1021/acs.langmuir.3c02185
Langmuir 2023, 39, 14764−14773

were used. Besides water and ethylene glycol (EG), three different solutions by volume of water and propylene glycol (PG) were employed, and their respective properties ($\mu$, $\rho$, and $\sigma$) are listed in Table 1. The viscosity of each of the PG−water mixtures was measured in a rheometer (TA Instruments AR 2000) with controlled stress and controlled shear rate operation, and the surface tension was obtained from measurement in a constant-bubble pressure tensiometer (SensaDyne QC6000). Several measurements were made in each case to ensure repeatable accuracy and verified with standard NIST (National Institute of Standards and Technology) properties; the density was taken from the latter's online resource.[34]

## RESULTS AND DISCUSSION

In order to understand the postimpact outcome behavior (deposition or splash) of drops impinging on a thin film of the same liquid, results of controlled experiments using high-resolution, high-speed digital video image capture and processing are presented. A substantive issue, as outlined in the introductory section, is to understand the underlying aspects of the disparities among previous studies and their respective bounds for the outcomes of the drop impact and to predict the onset of splashing. A comparison of the data from the current study for ($H^* = h/d$) = 0.1 with reported correlations[23,26,27] is graphed in Figure 5. Both splash and no-splash (or drop deposition) events at impact are appropriately identified to ascertain their efficacy. The considerable disagreement with predictions of these correlations, which are of the form $We\ Oh^{-0.4} = K$, where $1812 \leq K \leq 2500$ has a ~38% variation, over the full spectrum of $10^{-3} \leq Oh \leq 10^{-1}$, is evident. So is the case with the suggestion[28] that the critical Weber number is constant (or implicitly unique) for each $Oh$, or $We_c = C(Oh)$. This suggests that $We$ and $Oh$ are perhaps inadequate in scaling the splash-deposition event boundary.

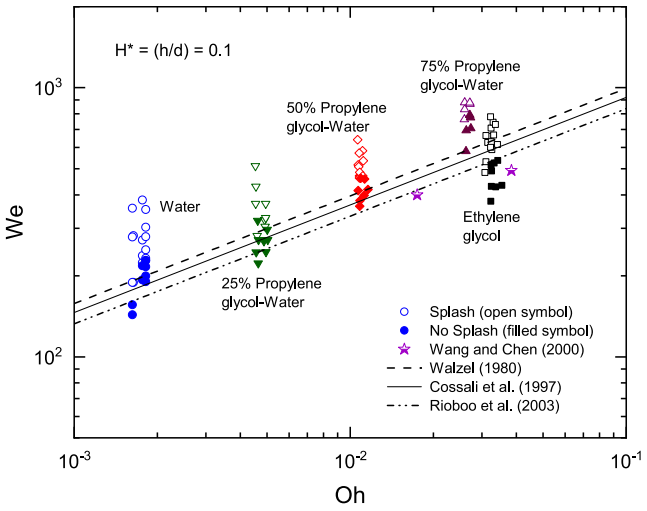


**Figure 5.** Comparison of experimental data for $H^* = 0.1$ with previously published correlations, of the form ($We = K{\cdot}Oh^{0.4}$), for predicting the demarcation between the droplet splash and nonsplash events.

The onset of almost all splashing events observed in the present experiments and depending on $Oh$ are seen to be under- or overpredicted; some deposition events too are underpredicted. It may be recalled that $K$ has previously been reported as constant (for $0.06 < H^* < 0.15$) and a function of film thickness (for $H^* < 0.06$) in one case[23] and as $K(H^*)$ for $H^* \geq 0.1$ in another study.[27] Moreover, overlapping data points for splash and deposition are incompatible with the $We_c = C(Oh)$ contention.[28] Very closely spaced data points were obtained in this study in an effort to better ascertain the onset of droplet splashing for each liquid on their respective thin film ($H^* = 0.1$). Nonetheless, considerable overlap between splash and deposition event points is observed in several cases. Perhaps $We$ and $Oh$ (and potentially $Re$ and $Oh$, as per eq 4), which consider the interaction of drop inertia with liquid surface tension and viscosity, do not completely scale the phenomena, and a careful re-evaluation is needed.

In order to identify all relevant scaling forces that influence the onset of drop-splash on a thin liquid film, the effects of different working liquid properties on the drop impact on the film surface are carefully evaluated. As the time-evolution images in Figure 6 reveal, the occurrence of four different phenomena in the splash and deposition (or no-splash) process can be discerned. Results for water droplets for four different conditions with $10{,}100 \geq Re \geq 5{,}709$, $308 \leq We \leq 86$, impacting a thin film ($H^* = 0.1$), are presented. The images in Figure 6a,b show postdrop-impact splashing, whereas those in Figure 6c,d show deposition events. While the respective end outcomes in the two pairs of events are the same, there are distinct differences in each case that merit closer scrutiny.

As the drop impacts the thin film surface, at the instant of impact, thin ejected jets emitting secondary drops produce a splash. This is emblematic of prompt splash and its progression is seen in Figure 6a. The ejected jet formed at impact resembles a crown as it continues to expand. The capillary surface waves formed on the crown create fingers at its periphery that extend upward, giving it this distinct structure; the growing fingers then break up or pinch off to form the secondary drops. As seen in Figure 6a, while the prompt splash occurs within 0.002 s of the drop impact, the fingers of the crown grow and ultimately break up into secondary drops after 0.14 s while falling back onto the thin film layer. The case in Figure 6b is a delayed or crown splash (or absence of prompt splash). A crown is first seen to form after impact and capillary waves begin to develop on its surface, which eventually can be seen to propagate and form fingers that break up at 0.012 s. Moreover, during crown splash, the secondary droplets are observed to be much larger and more uniform in comparison to those formed during prompt splash.

The two cases in Figure 6c,d are examples of deposition, but each with very distinct features. As evidenced in Figure 6c, the capillary surface waves formed at impact at 0.002 s are seen to propagate and form fingers of the crown. These fingers, however, do not further break up into drops but collapse into the crown before deposition on the thin liquid film. The case in Figure 6d, on the other hand, shows that the drop deposits on the thin film layer without forming any capillary waves on impact (0.002 s). Minor surface undulations are observed at 0.01 s, but they do not evolve to form finger-like structures before deposition. Accordingly, the two instances of deposition presented in Figure 6c,d, respectively, can be classified as two different types: fingered and nonfingered deposition. Closer inspection of the drop-impact event in Figure 6c with respect to those in Figure 6a,b, reveals that both an increase in diameter and an increase in impact velocity affect droplet splashing on a thin film. The diameter of the resulting crown on the thin film is seen to be a function of the drop diameter. So, for the same velocity of impact, a smaller drop results in a smaller crown diameter with a lower degree of splashing, as in


https://doi.org/10.1021/acs.langmuir.3c02185
Langmuir 2023, 39, 14764−14773

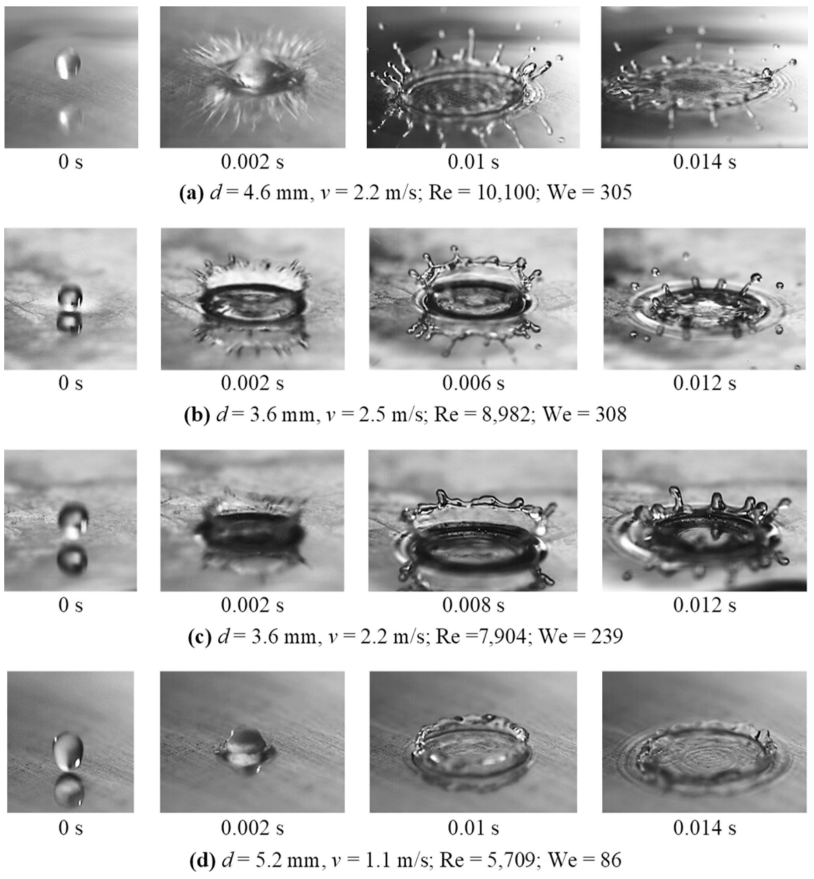


**Figure 6.** Time-progression images of splash or deposition events for a water drop of different diameter $d$ impacting on a thin water film ($H^* = 0.1$) with different velocity $v$ ($10{,}100 \geq Re \geq 5709$; $308 \geq We \geq 86$).

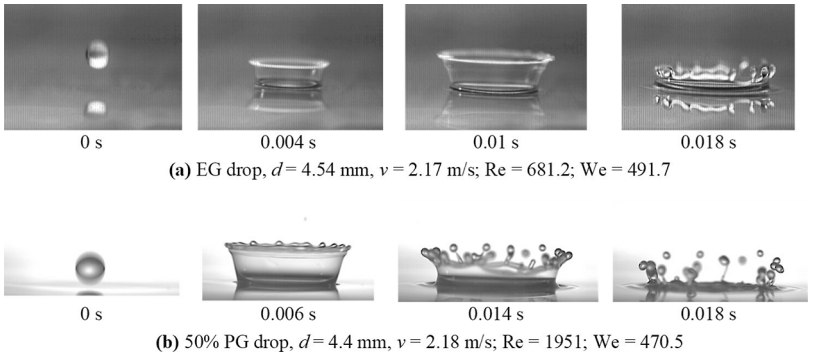


**Figure 7.** Time-progression images of splash events for two different fluid drops upon impingement on their respective liquid thin water films ($H^* = 0.1$): (a) EG drop on its film and (b) 50% PG drop on its film.

Figure 6a,c; for the same drop diameter, a larger velocity results in splashing, as contrasted by that seen in Figure 6b from the deposition in Figure 6c. The effective scaling of the inherent drivers of these distinct postdrop-impact events with water also needs fluid-dependent evaluation.

For resolving the influence of different forces on the splashing-deposition phenomena, the effect of liquid properties also needs to be understood in addition to the drop size and its impact velocity. It is postulated that the spread of the impacting drop primarily receives resistance from the thin film and that the postimpact instantaneous base of the crown has a velocity comparable to the impact velocity. While initially it assists in the growth of the crown base, this velocity decreases with subsequent crown development until the crown finally collapses on the thin liquid film. The decrease in this velocity of the crown base can therefore be related to the resistance offered by the liquid and, hence, the viscous property of the liquid.

To characterize viscous effects, images of postimpact time progression events with same-sized drops of two different liquids (EG and 50% PG) impacting their respective thin films ($H^* = 0.1$) with similar velocities are presented in Figure 7. With nearly the same $We$ in these two cases, their substantially different $Res$ manifest the viscous resistance offered to the drop-impact inertia. The rim of the crown that forms at 0.004 s with an EG drop-film (Figure 7a) is observed to remain uniform and have no undulations. Instability on the crown rim is not seen until it begins to collapse during deposition at 0.018


https://doi.org/10.1021/acs.langmuir.3c02185
Langmuir 2023, 39, 14764−14773

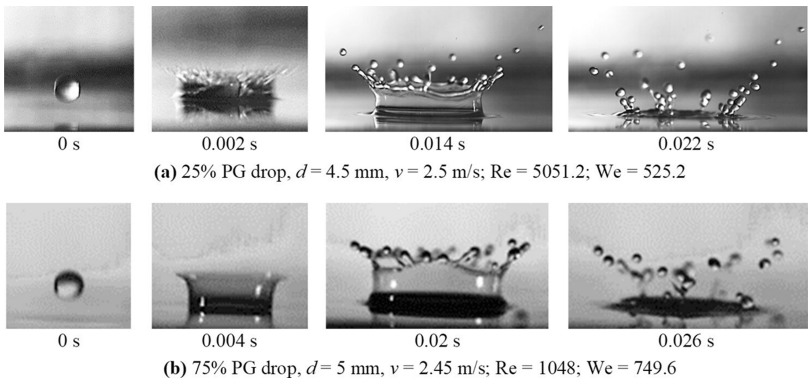


**(a)** 25% PG drop, $d$ = 4.5 mm, $v$ = 2.5 m/s; Re = 5051.2; We = 525.2

**(b)** 75% PG drop, $d$ = 5 mm, $v$ = 2.45 m/s; Re = 1048; We = 749.6

**Figure 8.** Time-progression images of splash events for two different fluid drops upon impingement on their respective liquid thin water films ($H^*$ = 0.1): (a) 25% PG drop on its film and (b) 75% PG drop on its film.

s. Contrastingly, in the case of 50% PG, minor surface waves are noticed at 0.006 s; these disturbances grow and ultimately result in a modest splash at 0.018 s. Even though the EG drop diameter is slightly larger (hence the small difference in *We*; 491.7 versus 470.5) than the 50% PG drop, the former does not splash. The viscosity of EG is nevertheless an order of magnitude higher than that of 50% PG, thereby offering a greater liquid-film resistance to the growing crown and suppressing splashing. This is reflected in their significantly different *Res* (681.2 for EG versus 1951 for 50% PG) and points to the limitation of the surface tension-based *We* in scaling the deposition-splash events on thin liquid films; *Re* is then a more appropriate scaling parameter, especially for the dominant viscous force effects.

Figure 8 further illustrates the interplay of viscosity and surface tension with the postimpact behavior of two liquid drops, one of 25% PG and the other of 75% PG, impinging on their respective thin liquid films ($H^*$ = 0.1). The impact velocities and drop diameters are about the same, and varying *Res* and *Wes* reflect different properties (primarily viscosity and surface tension) of the two water−glycol solutions. In the case of 25% PG, at 0.002 s (Figure 8a), the drop impact on its liquid film is seen to generate capillary waves. This disturbance is not seen in the immediate postimpact aftermath (at 0.004 s) crown of the 75% PG drop (Figure 8b). The delayed formation of capillary waves does eventually lead to the formation of fingers at the crown surface (Figure 8b at 0.02 s), by which time the fingers in the 25% PG crown have already broken up into secondary droplets (Figure 8a at 0.014 s); finger breakup to form droplets occurs much later in the 75% PG case. Moreover, a larger number of secondary drops after splashing occurs is formed in the 25% PG case.

As the liquid crown spreads after drop impingement on the thin liquid film, the instability on the rim leads to crown growth or upward stretching. Depending upon fluid properties, and potentially the interplay of viscous, surface, or interfacial tension and gravitational forces, finger formation develops in the crown, leading to the breakup of their elongating ends into secondary droplets. In this instability-driven crown breakup process, the surface energy (governed by the surface tension of the liquid) tends to decrease at the crown edges as the perimeter grows. This yields finger formation, its stretching or growth, and its breakup into secondary droplets. Crown and finger elongations, driven by reducing surface energy, tend to be retarded by gravitational and viscous forces. Correspondingly, with an order-of-magnitude lower viscosity but slightly higher surface tension of 25% PG as compared with that of 75% PG (see Table 1), breakup and drop splash occur more readily and extensively in the former case.

Based on these observations and as highlighted in the experimental results for the drop-splash and drop-deposition events on a thin liquid film (Figures 6−8), it is therefore hypothesized that (i) postdrop-impingement, the crown rim formation and its subsequent growth are governed by the interplay of the drop-impact inertia and the viscous force of the liquid, and (ii) the breakup of the crown rim into secondary drops is essentially dictated by the interplay of gravity and surface tension force acting to minimize surface energy at the expanding crown rim edge. While the relative interaction of inertial and viscous forces can be scaled by *Re*, as given in eq 4, the balance between gravitational and interfacial or surface tension forces is given by

$$\text{Bond number, } Bo = \left(\frac{\rho g d^2}{\sigma}\right) = \frac{\text{gravitational force}}{\text{surface tension or capillary force}} \tag{8}$$

Thus, the effectiveness of *Re* and *Bo* in defining the splashing threshold for drops impinging on their thin liquid film can be seen in the plot of Figure 9 with the current experimental data. It is observed that the demarcation of the deposition (no splash)−splash boundary can be represented by the following expression for each of the five liquids considered in this study

$$Re = C \cdot Bo^{0.1} \tag{9}$$

Note that the lead coefficient $C$ in eq 9 is dependent upon the droplet−film liquid system and is a function of its properties.

The scaling of the interplay of the fluid properties of density, surface tension, and viscosity can be described by the Morton number[30,31,35,36] that is expressed as

$$Mo = \left[\frac{g(\rho - \rho_a)\mu^4}{\rho^2\sigma^3}\right] \simeq \left(\frac{g\mu^4}{\rho\sigma^3}\right) \sim \frac{\text{gravitational (density) and viscous effects}}{\text{surface or interfacial tension effects}} \tag{10}$$



https://doi.org/10.1021/acs.langmuir.3c02185
Langmuir 2023, 39, 14764−14773

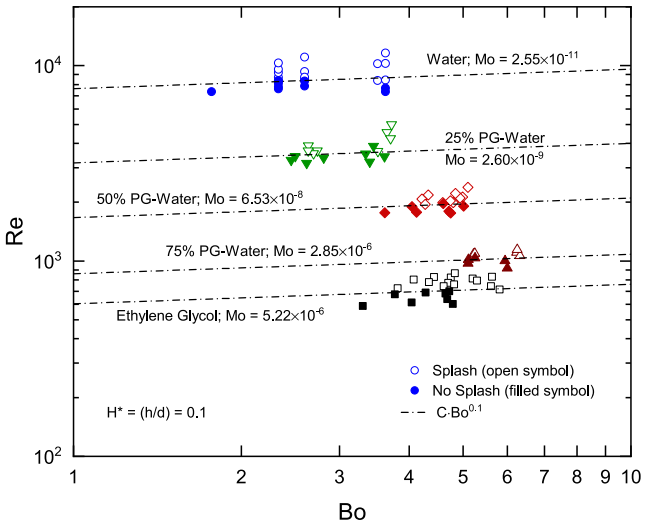


**Figure 9.** Variation of impinging-drop Reynolds number, *Re*, with Bond number, *Bo*, for different liquids characterized by their Morton number, *Mo*.

The functional relationship of $C$ with $Mo$ works out to $C = (60/Mo^{0.2})$, and hence, by combining this with eq 9, the following correlation is arrived at

$$Re = 60(Bo^{0.1}/Mo^{0.2}) \tag{11}$$

The efficacy of eq 11 in predicting the onset of a splash of drops in thin liquid films ($H^* \sim 0.1$) is evident in Figure 10. The experimental data of both the present work and those reported in the literature[28,29] are seen to be very well represented. It must be noted, however, that while this correlation and data are for $H^* \sim 0.1$, its validity and applicability may be extended to even thinner liquid films ($0.05 > H^* \leq 0.1$) if we accept the findings and contention of Wang and Chen[28] and Rioboo et al.[23] that the critical splash threshold *We* is the same in this range. In other words, for a given fluid system, the limiting drop diameter $d$ and its impact velocity $v$ are the same for splashing to occur in this liquid film thickness range; however, smaller $d$ and/or $v$ would lead to this outcome when $H^* < 0.05$. Both *Re* (as the predictor in eq 11) and *We* have $d$ and $v$ as the two primary variables besides fluid properties.

Furthermore, an important difference in the present scaling and correlation development is that the effects of the gravitational force are not neglected, unlike most previous studies.[23,27−29] For instance, while Cossali et al.[27] indicated that postimpact, gravity force may act in a manner similar to surface forces in the crown propagation, only the opposing surface and inertial forces along with viscous damping were considered as primary propagation drivers. Perhaps the issue stems from using a film thickness-based $Bo_h$, which was small ($0.12 < Bo_h < 1.2$), as the predictor for their data and thus neglecting this force. For the drop diameter-based definition as per eq 8 and for $H^* = 0.1$, these data would be in the larger range of $1.2 < Bo < 12$. Most of the subsequent studies have likewise ignored this in following the prevailing ($We/Oh^{0.4}$) scaling, despite larger *Bo* in their respective data set. This is in the range of $3.07 < Bo < 3.98$ in the case of Wang and Chen[28] and $0.09 < Bo < 4.48$ for Rioboo et al.;[23] the latter is based on the limited minimum and maximum drop diameters listed, which obviates comparison with present results. In the current study, the data are in the range $1.5 < Bo < 7.0$, and interestingly, as seen in Figure 10, besides the large-*Bo* data of Wang and Chen,[28] those of Vander Wal et al.,[29] with smaller values ($0.54 < Bo < 1.19$), also agree with the correlation of eq 11. The latter thus provides a good prediction for drop-splash thresholds for a reasonably wide range of *Bo* and thin films ($H^*$).

## CONCLUSIONS

An experimental investigation of drop-impact dynamics on thin liquid films is carried out. Five different liquids, including water, are considered in order to cover a wide range of fluid properties and to understand their effect on the postimpact splash-deposition behavior. Using high-speed high-resolution real-time image capture and processing, postimpact drop−film developments and a range of drop diameters and impact velocities are considered while maintaining the dimensionless film height of $H^* = 0.1$. The experimental data and its analysis are interesting and provide new insights into the postimpact splash-deposition phenomenon and highlight the inadequacy of the hitherto employed ($We/Oh^{0.4}$) grouping to predict the intervening threshold. In fact, there is no agreement on the quantification of this scaling, and 38% variance is seen in

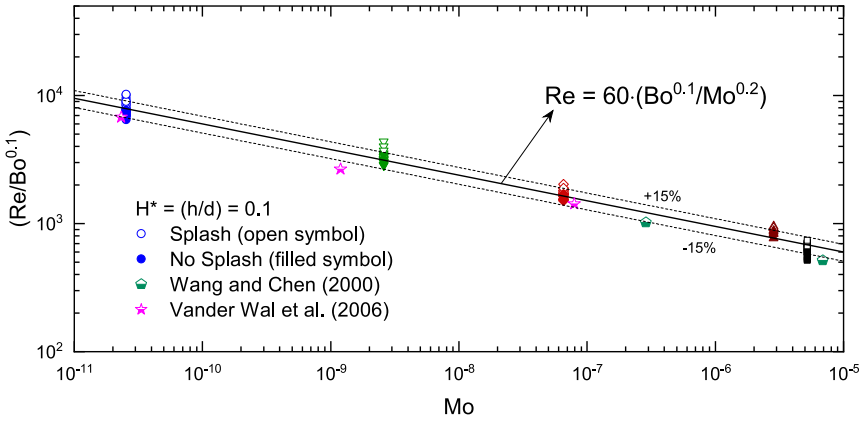


**Figure 10.** Comparison of predictions of correlation, given by eq 11, with experimental data for the splash-deposition threshold boundary for a drop impinging upon a thin film ($H^* = 0.1$) in different *Mo* liquid systems (note that for Wang and Chen[28] and Vander Wal et al.,[29] the data are for the "critical" or demarcating boundary value reported in each case).



https://doi.org/10.1021/acs.langmuir.3c02185
Langmuir 2023, 39, 14764−14773

Figure 2; there is predictive disagreement (Figure 5) with the results of the present study as well.

The observed interplay of liquid properties, specifically viscosity and surface tension, apart from contributions of the drop diameter and impact velocity, yields two important hypotheses: (i) a drop impacting a thin film encounters viscous resistance at the drop−film interface as it spreads along the film and the ejected displaced fluid begins to form a crown and (ii) surface tension of the liquid tends to minimize the surface energy at the crown rim and, balanced by the gravitational force, it affects the potential rim breakup and production of ejecting secondary drops. In the first instance, the primary driving force for the postdrop-impact dynamics, or the drop inertia, and the viscous resistance to its initial spread from the liquid film are shown to scale with *Re*. The subsequent gravitational and interfacial tension interactions during the crown formation and its possible breakup are found to scale with *Bo*. Moreover, the effect of variations in fluid properties is shown to be characterized by their *Mo*. Based on this scaling and analysis of the experimental data, a predictive correlation is devised, as expressed in eq 11, for demarcating the onset of splash when a drop impacts a thin liquid film ($H^* \leq 0.1$). Its predictions are seen to also agree well with data from several past experimental studies[28,29]. As such, this correlation would be quite useful for designing more effective spray-coating systems for a variety of fluids (*Mo*), predicting splash-caused chemical-laden liquid pollution, and, thereby, devising operative protocols for mitigating health risks, among many other similar applications.

## AUTHOR INFORMATION


### Corresponding Author

**R. M. Manglik** − *Thermal-Fluids and Thermal Processing Laboratory, Department of Mechanical and Materials Engineering, University of Cincinnati, Cincinnati, Ohio 45221-0072, United States;* orcid.org/0000-0001-7336-329X; Email: Raj.Manglik@uc.edu

### Authors

**S. Rajendran** − *Thermal-Fluids and Thermal Processing Laboratory, Department of Mechanical and Materials Engineering, University of Cincinnati, Cincinnati, Ohio 45221-0072, United States*

**M. A. Jog** − *Thermal-Fluids and Thermal Processing Laboratory, Department of Mechanical and Materials Engineering, University of Cincinnati, Cincinnati, Ohio 45221-0072, United States;* orcid.org/0000-0001-8334-8472

Complete contact information is available at: https://pubs.acs.org/10.1021/acs.langmuir.3c02185


### Notes

The authors declare no competing financial interest.

## ACKNOWLEDGMENTS

This research study was partially supported by the National Institute for Occupational Safety and Health (NIOSH) Pilot Research Project Training Program of the University of Cincinnati Education and Research Center and grant #T42/OH008432-08.

## NOMENCLATURE

*Bo*, Bond number ($=\rho g d^2/\sigma$); *d*, impacting drop diameter [m]; *g*, gravitational acceleration [m/s$^2$]; *h*, liquid film thickness of substrate [m]; $H^*$, dimensionless liquid film thickness($=h/d$); *v*, drop velocity near surface or film impact [m/s]; *Mo*, Morton number ($=g\mu^4/\rho\sigma^3$); *Oh*, Ohnesorge number ($=\mu/\sqrt{\rho\sigma d} = \sqrt{\mathrm{We}}/\mathrm{Re}$); *Re*, Reynolds number ($=\rho v d/\mu$); *We*, Weber number ($=\rho v^2 d/\sigma$); $\mu$, dynamic viscosity of the liquid [Pa s]; $\rho$, density of the liquid [kg/m$^3$]; $\sigma$, surface tension of the liquid [N/m]

## REFERENCES


(1) Semanová, P.; Kučera, M. Health Effects from Occupational Exposure to Metalworking Fluid Mist. *Key Eng. Mater.* **2013**, *581*, 112−118.

(2) Gunter, K. L.; Sutherland, J. W. An Experimental Investigation into the Effect of Process Conditions on the Mass Concentration of Cutting Fluid Mist in Turning. *J. Clean. Prod.* **1999**, *7* (5), 341−350.

(3) Worthington, A. M. On the Forms Assumed by Drops of Liquids Falling Vertically on a Horizontal Plate. *Proc. Roy. Soc. Lond.* **1876**, *25* (1876−1877), 261−272.

(4) Chandra, S.; Avedisian, C. T. On the Collision of a Droplet with a Solid Surface. *Proc. R. Soc. A* **1991**, *432* (1884), 13−41.

(5) Asai, A.; Shioya, M.; Hirasawa, S.; Okazaki, T. Impact of an Ink Drop on Paper. *J. Imaging Sci. Technol.* **1993**, *37* (2), 205−207.

(6) Yarin, A. L.; Weiss, D. A. Impact of Drops on Solid Surfaces: Self-Similar Capillary Waves, and Splashing as a New Type of Kinematic Discontinuity. *J. Fluid Mech.* **1995**, *283*, 141−173.

(7) Mao, T.; Kuhn, D. C. S.; Tran, H. Spread and Rebound of Liquid Droplets upon Impact on Flat Surfaces. *AIChE J.* **1997**, *43* (9), 2169−2179.

(8) Rioboo, R.; Tropea, C.; Marengo, M. Outcomes from a Drop Impact on Solid Surfaces. *Atomization Sprays* **2001**, *11* (2), 12−165.

(9) Šikalo, Š.; Marengo, M.; Tropea, C.; Ganic, E. N. Analysis of Impact of Droplets on Horizontal Surfaces. *Exp. Therm. Fluid Sci.* **2002**, *25*, 503−510.

(10) Gatne, K. P.; Manglik, R. M.; Jog, M. A. Visualization of Fracture Dynamics of Droplet Recoil on Hydrophobic Surface. *ASME J. Heat Mass Transfer* **2007**, *129* (8), 931.

(11) Gatne, K. P.; Jog, M. A.; Manglik, R. M. Surfactant Induced Modification of Low Weber Number Droplet Impact Dynamics. *Langmuir* **2009**, *25* (14), 8122−8130.

(12) Ravi, V.; Jog, M. A.; Manglik, R. M. Effects of Pseudoplasticity on Spread and Recoil Dynamics of Aqueous Polymeric Solution Droplets on Solid Surfaces. *Interfacial Phenom. Heat Transf.* **2013**, *1* (3), 273−287.

(13) Manglik, R. M.; Jog, M. A.; Gande, S. K.; Ravi, V. Damped Harmonic System Modeling of Post-Impact Drop-Spread Dynamics on a Hydrophobic Surface. *Phys. Fluids* **2013**, *25* (8), 082112.

(14) Breitenbach, J.; Roisman, I. V.; Tropea, C. From Drop Impact Physics to Spray Cooling Models: A Critical Review. *Exp. Fluid* **2018**, *59* (3), 55.

(15) Burzynski, D. A.; Roisman, I. V.; Bansmer, S. E. On the Splashing of High-Speed Drops Impacting a Dry Surface. *J. Fluid Mech.* **2020**, *892*, A2.

(16) Okawa, T.; Kubo, K.; Kawai, K.; Kitabayashi, S. Experiments on Splashing Thresholds During Single-Drop Impact onto a Quiescent Liquid Film. *Exp. Therm. Fluid Sci.* **2021**, *121*, 110279.

(17) Mundo, C.; Sommerfeld, M.; Tropea, C. On the Modeling of Liquid Sprays Impinging on Surfaces. *Atomization Sprays* **1998**, *8* (6), 625−652.

(18) Trujillo, M. F.; Lee, C. F. Modeling Crown Formation due to the Splashing of a Droplet. *Phys. Fluids* **2001**, *13* (9), 2503−2516.

(19) Gunjal, P. R.; Ranade, V. V.; Chaudhari, R. V. Dynamics of drop impact on solid surface: Experiments and VOF simulations. *AIChE J.* **2005**, *51* (1), 59−78.

(20) Cimpeanu, R.; Papageorgiou, D. T. Three-Dimensional High Speed Drop Impact onto Solid Surfaces at Arbitrary Angles. *Int. J. Multiphase Flow* **2018**, *107*, 192−207.
(21) Fest-Santini, S.; Steigerwald, J.; Santini, M.; Cossali, G. E.; Weigand, B. Multiple Drops Impact onto a Liquid Film: Direct Numerical Simulation and Experimental Validation. *Comput. Fluids* **2021**, *214* (1), 104761.
(22) Yarin, A. L. Drop Impact Dynamics: Splashing, Spreading, Receding, Bouncing. *Annu. Rev. Fluid. Mech.* **2006**, *38*, 159−192.
(23) Rioboo, R.; Bauthier, C.; Conti, J.; Voué, M.; De Coninck, J. Experimental Investigation of Splash and Crown Formation during Single Drop Impact on Wetted Surfaces. *Exp. Fluid* **2003**, *35* (6), 648−652.
(24) Josserand, C.; Zaleski, S. Droplet splashing on a thin liquid film. *Phys. Fluids* **2003**, *15* (6), 1650−1657.
(25) Deegan, R. D.; Brunet, P.; Eggers, J. Complexities of Splashing. *Nonlinearity* **2008**, *21* (1), C1−C11.
(26) Walzel, P. Zerteilgrenze beim Tropfenprall. *Chem. Ing. Tech.* **1980**, *52* (4), 338−339.
(27) Cossali, G. E.; Coghe, A.; Marengo, M. The Impact of a Single Drop on a Wetted Solid Surface. *Exp. Fluid* **1997**, *22* (6), 463−472.
(28) Wang, A. B.; Chen, C. C. Splashing Impact of a Single Drop onto Very Thin Liquid Films. *Phys. Fluids* **2000**, *12* (9), 2155−2158.
(29) Vander Wal, R. L.; Berger, G. M.; Mozes, S. D. Droplets Splashing upon Films of the Same Fluid of Various Depths. *Exp. Fluid* **2006**, *40*, 33−52.
(30) Clift, R.; Grace, J. R.; Weber, M. E. *Bubbles, Drops, and Particles*; Academic Press: New York, NY, 1978.
(31) Sadhal, S. S.; Ayyaswamy, P. S.; Chung, J. N. *Transport Phenomena with Drops and Bubbles*; Springer: New York, NY, 1997.
(32) Okawa, T.; Shiraishi, T.; Mori, T. Production of Secondary Drops During the Single Water Drop Impact onto a Plane Water Surface. *Exp. Fluid* **2006**, *41*, 965−974.
(33) Coppola, G.; Rocco, G.; de Luca, L. Insights on the Impact of a Plane Drop on a Thin Liquid Film. *Phys. Fluids* **2011**, *23* (2), 022105.
(34) NIST. Chemistry WebBook, SRD 69, https://webbook.nist.gov/chemistry/fluid/. National Institute of Standards and Technoloy: Washington, DC, 2023 (accessed July 20, 2022).
(35) Pfister, M.; Hager, W. H. History and Significance of the Morton Number in Hydraulic Engineering. *J. Hydraul. Eng.* **2014**, *140* (5), 02514001.
(36) Haberman, W. L.; Morton, R. K. *An Experimental Investigation of the Drag and Shape of Air Bubbles Rising in Various Liquids*; US Navy, The David W. Taylor Model Basin: Washington, DC, 1953; Report No. 802, NS 715−102.



https://doi.org/10.1021/acs.langmuir.3c02185
*Langmuir* 2023, 39, 14764−14773